Supporting information

Stretchable Mesoporous Electrodes as a Versatile Platform for Minimally Invasive Surgical Devices

Michael Abraham Listyawan[1], Chi Cong Nguyen[1], Tran Bach Dang[1], Nhat Mihn Doan[1], Quang Ahn Nguyen[1], Yulin Qiu[1,2], Eva Tomaskovic-Crook[4,5,6], Mostafa Kamal Masud[3], Yusuke Yamauchi[3], Jeremy Micah Crook[4,5,6], Mohit Naresh Shivdasani[2], Thanh Nho Do[2,7], Hoang-Phuong Phan[1,7]*

[1]*School of Mechanical and Manufacturing Engineering, The University of New South Wales, Sydney, NSW 2052, Australia*

[2]*Graduate School of Biomedical Engineering, The University of New South Wales, Sydney, NSW 2052, Australia*

[3]*Australian Institute of Bioengineering and Nanotechnology (AIBN) and School of Chemical Engineering, The University of Queensland, St Lucia, QLD 4072, Australia*

[4]*Arto Hardy Family Biomedical Innovation Hub, Chris O'Brien Lifehouse, Camperdown, NSW, 2050 Australia*

[5]*School of Medical Sciences, Faculty of Medicine and Health, The University of Sydney, Camperdown, NSW, 2006 Australia*

[6]*Intelligent Polymer Research Institute, Innovation Campus, University of Wollongong, Squires Way, Fairy Meadow, NSW, 2519 Australia*

[7]*Tyree Foundation Institute of Health Engineering, University of New South Wales, Sydney, NSW 2052, Australia*

Email: hp.phan@unsw.edu.au

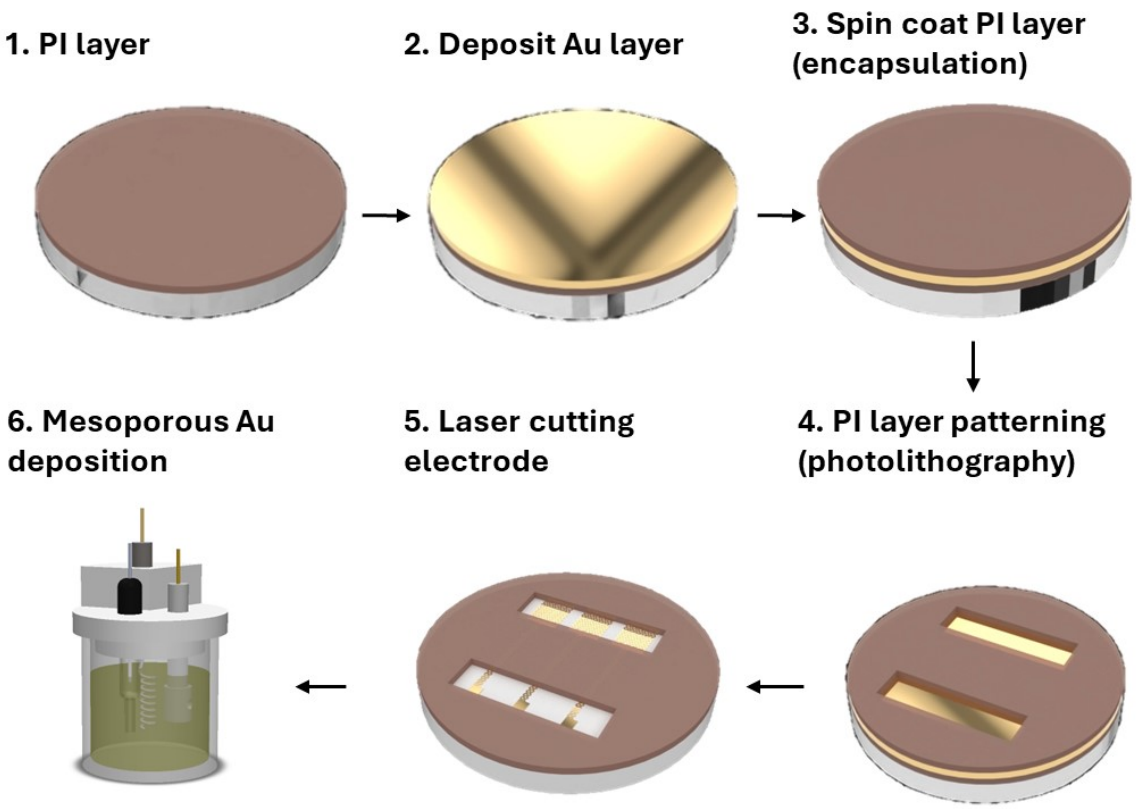

Figure S1 Fabrication steps of the flexible mesoporous gold electrode

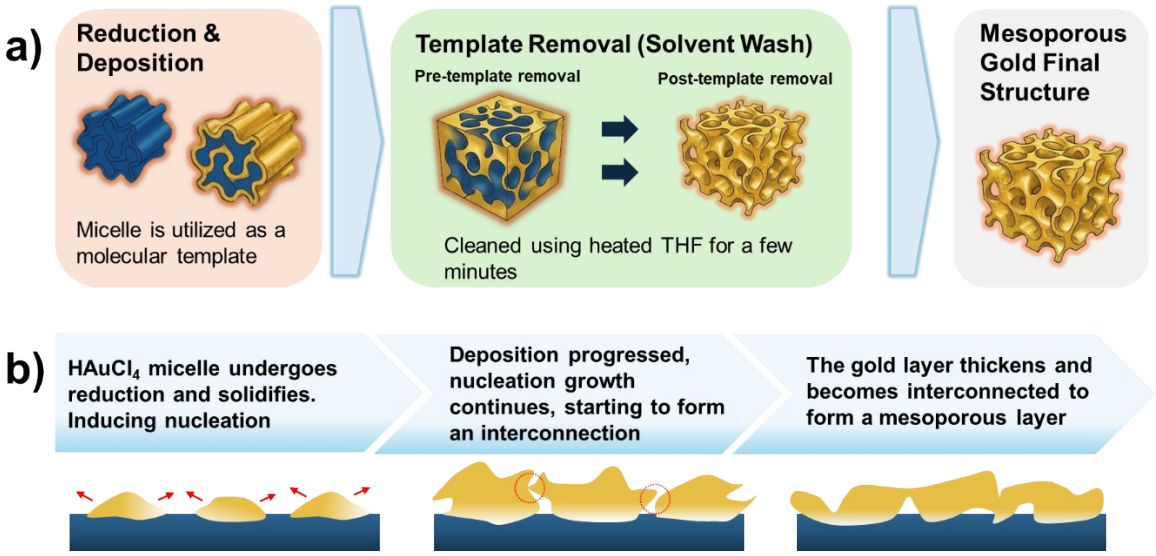

Figure S2 Schematic of mesoporous gold overall process and growth mechanisms. (a) The overall process that occurs on the mesoporous gold layer during deposition and post-deposition. (b) The growth mechanisms of the mesoporous gold layer during deposition.

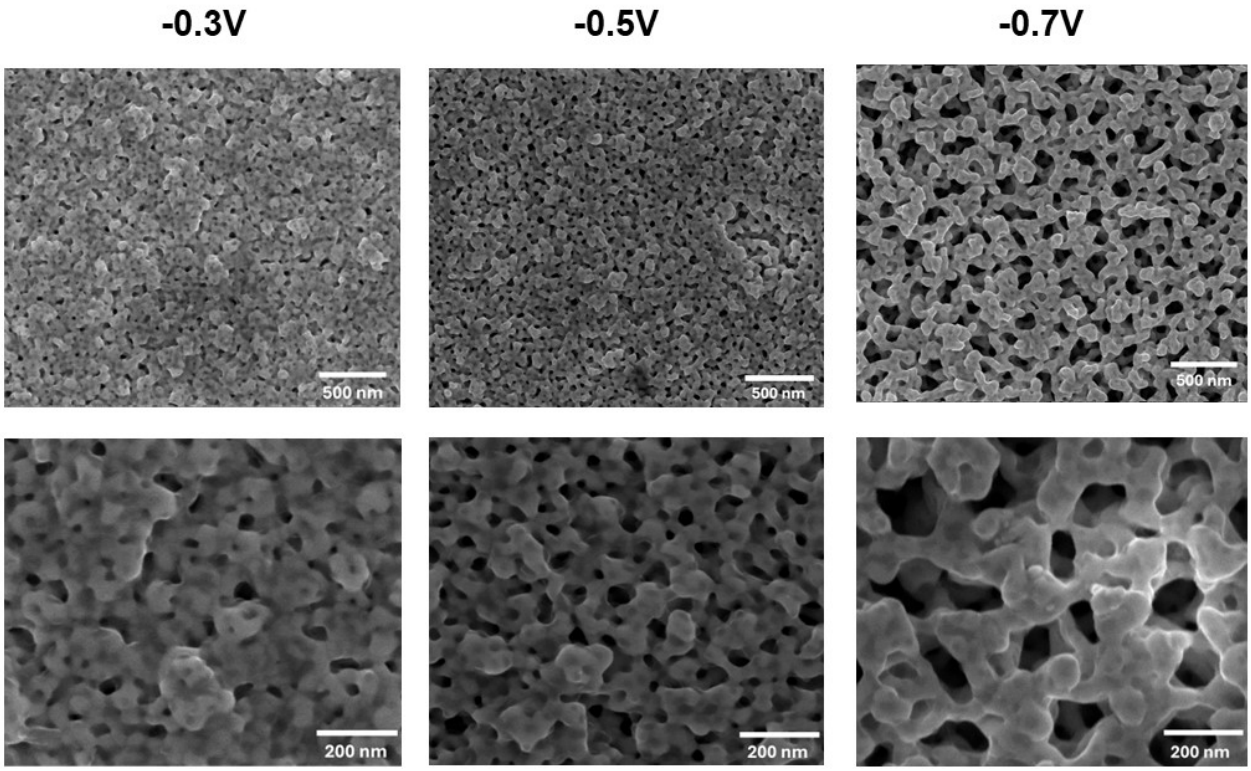

Figure S3 SEM micrographs of mesoporous gold under various voltages applied

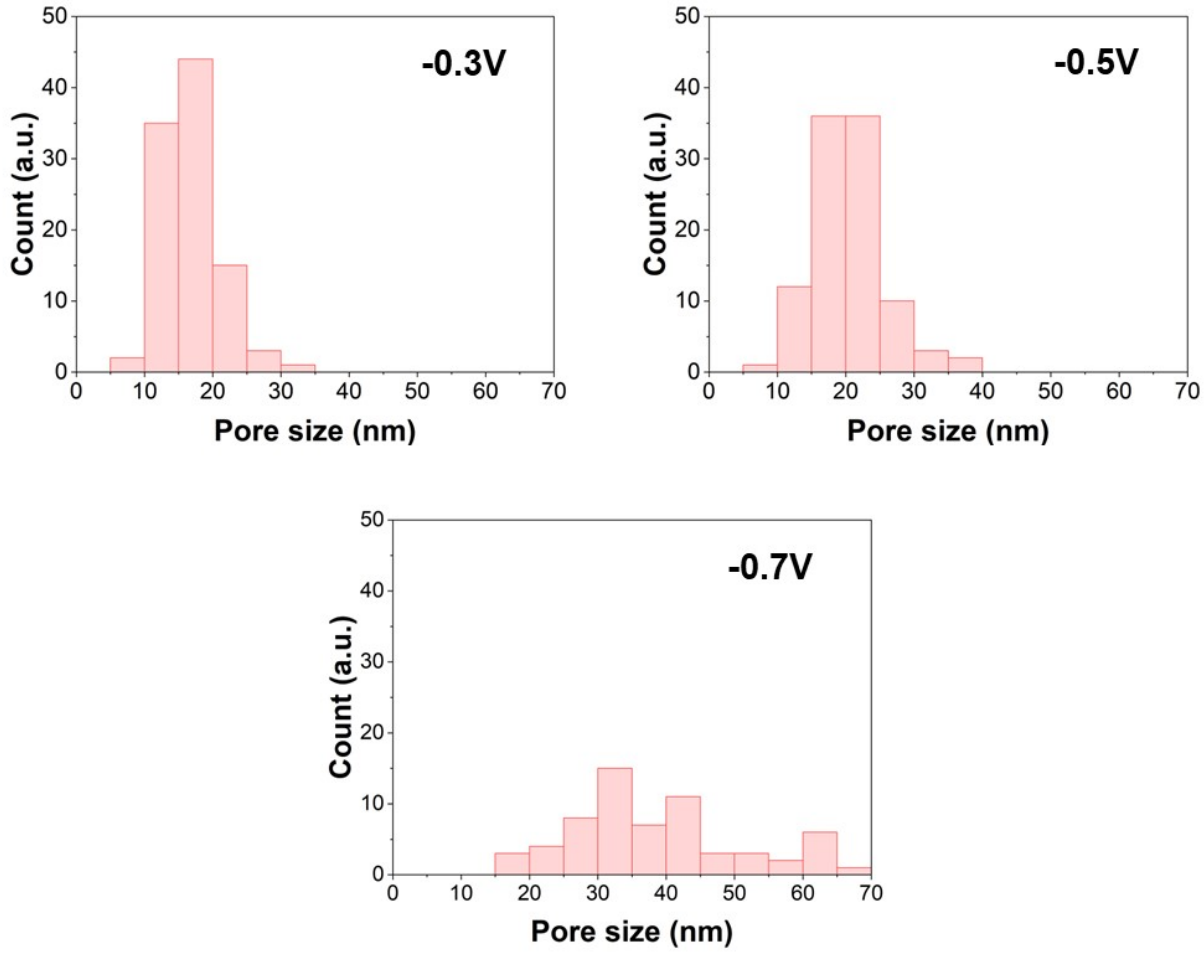

Figure S4 Pore size distribution of mesoporous gold under different voltages applied during deposition.

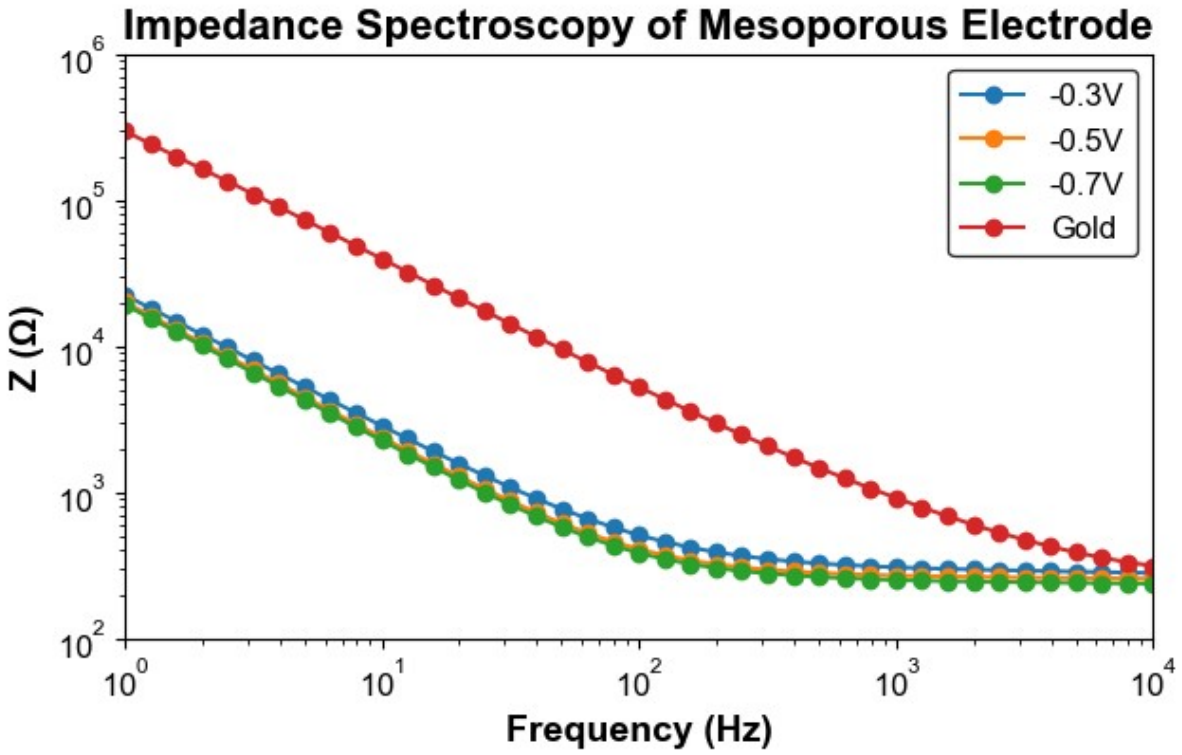

Figure S5 Electrochemical impedance spectroscopy (EIS) of mesoporous gold under various voltages applied during mesoporous gold layer deposition (-0.3V, -0.5V, -0.7V).

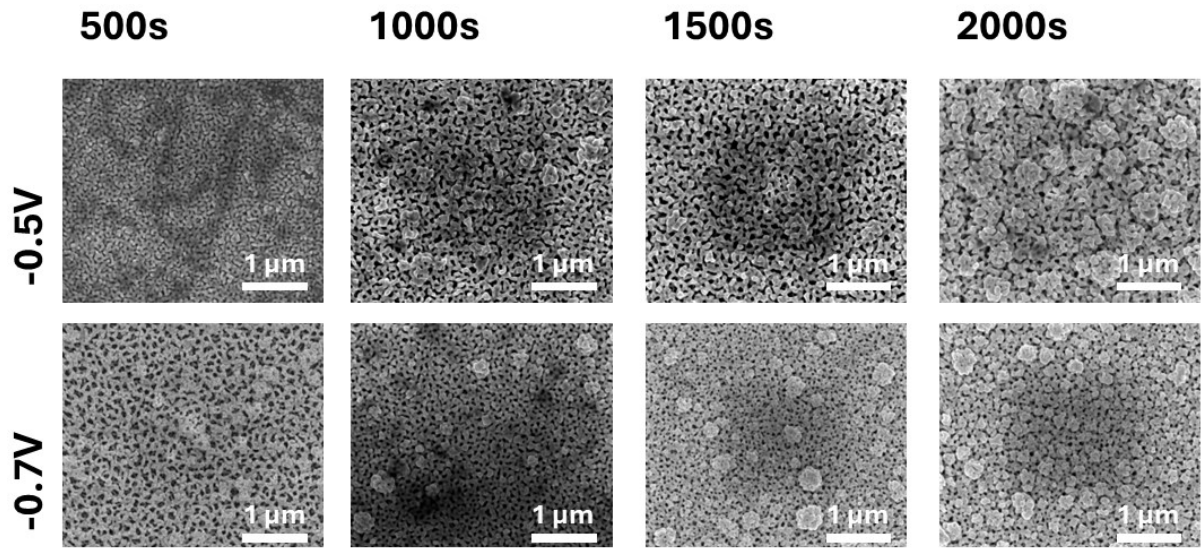

Figure S6 SEM micrographs of mesoporous gold under different voltages and deposition durations

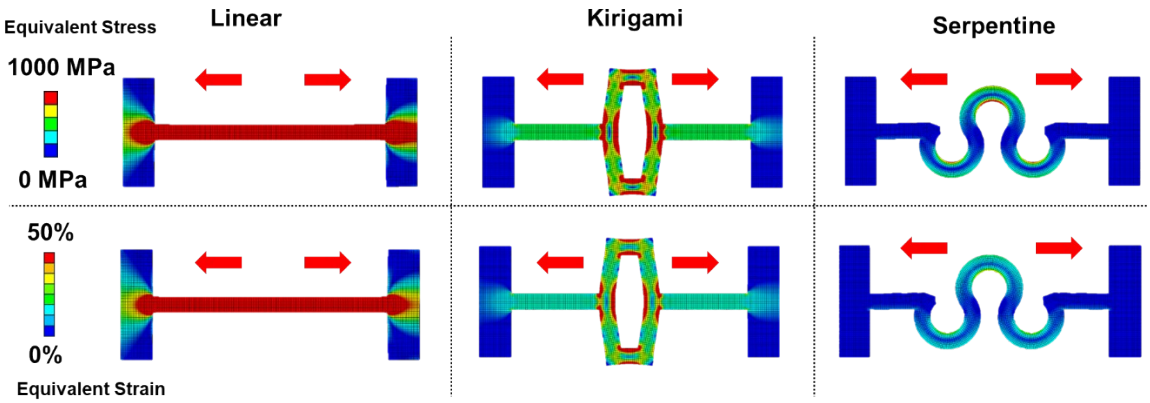

Figure S7 FEA simulation comparison of linear, kirigami, and serpentine structures with the gage length of 1.4 mm and applied displacement of 1.4 mm.

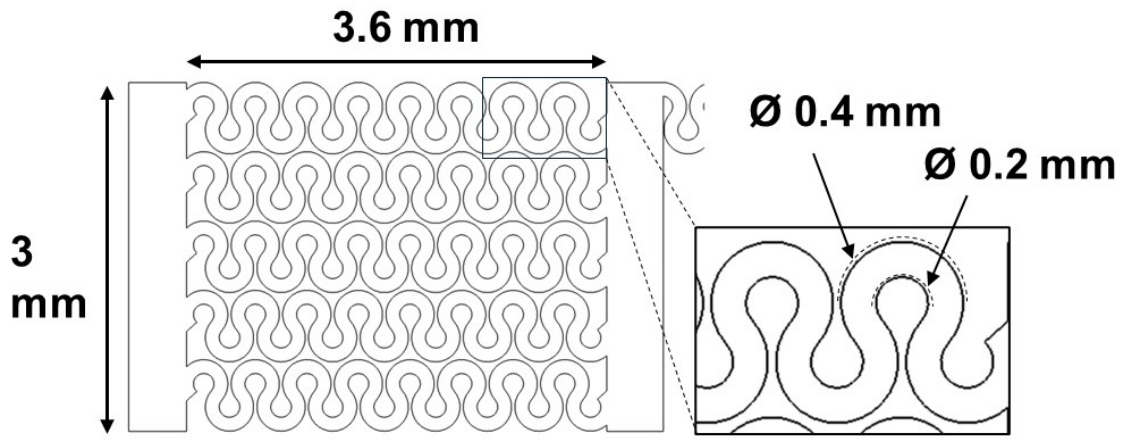

Figure S8 Flexible serpentine electrode dimensions with serpentine inner and outer diameter.

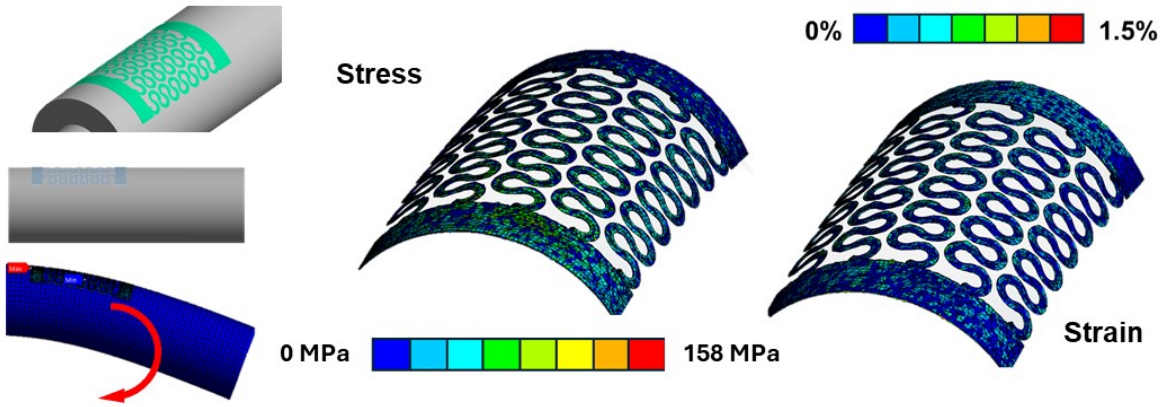

Figure S9 FEA simulation when the model is applied with a bending motion. The bending motion is visualized, and its stress and strain distribution map.

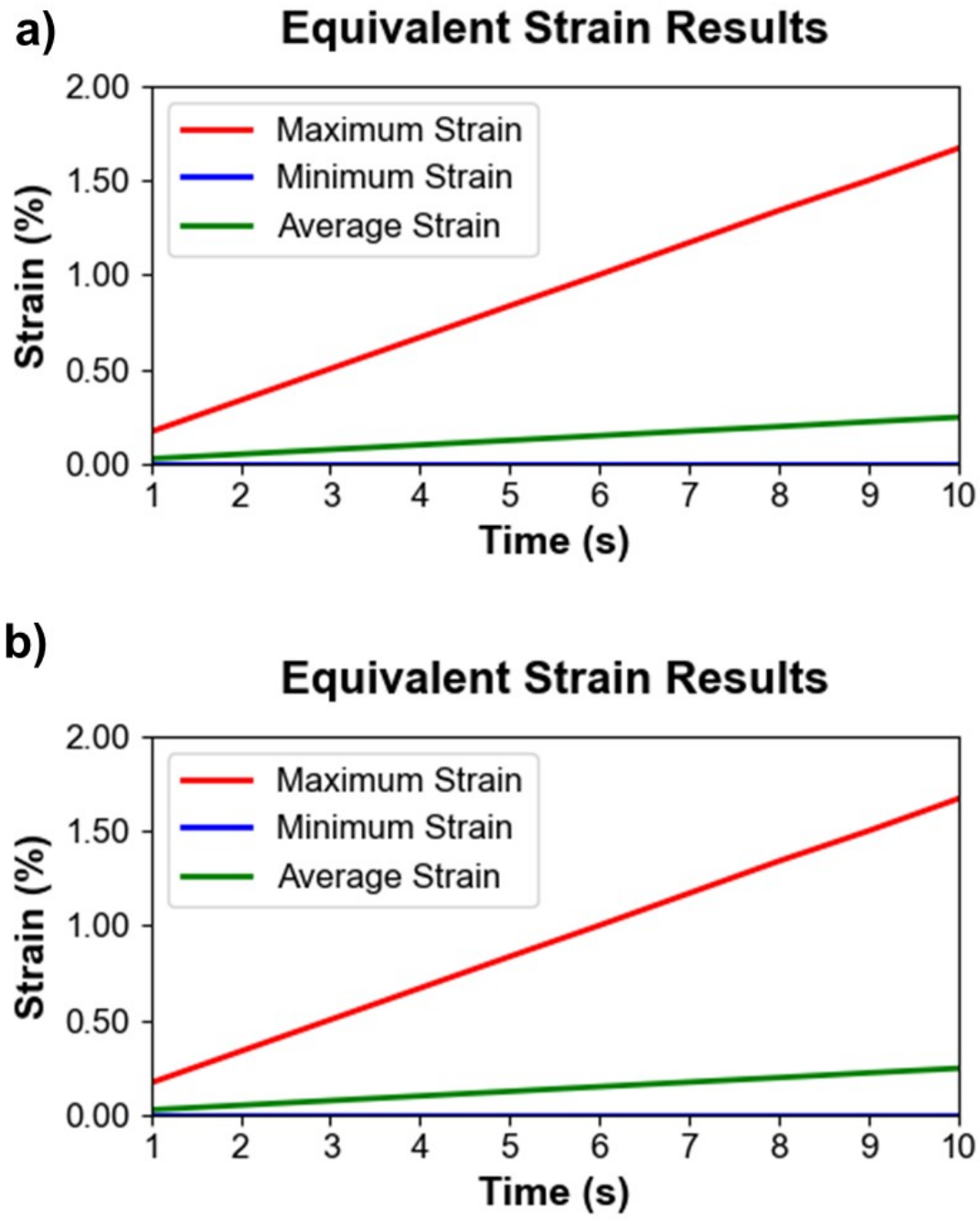

Figure S10 Stress and Strain results from FEA simulations when applied with a bending moment for 10 split substeps, showing the maximum, minimum, and average value of each substep.

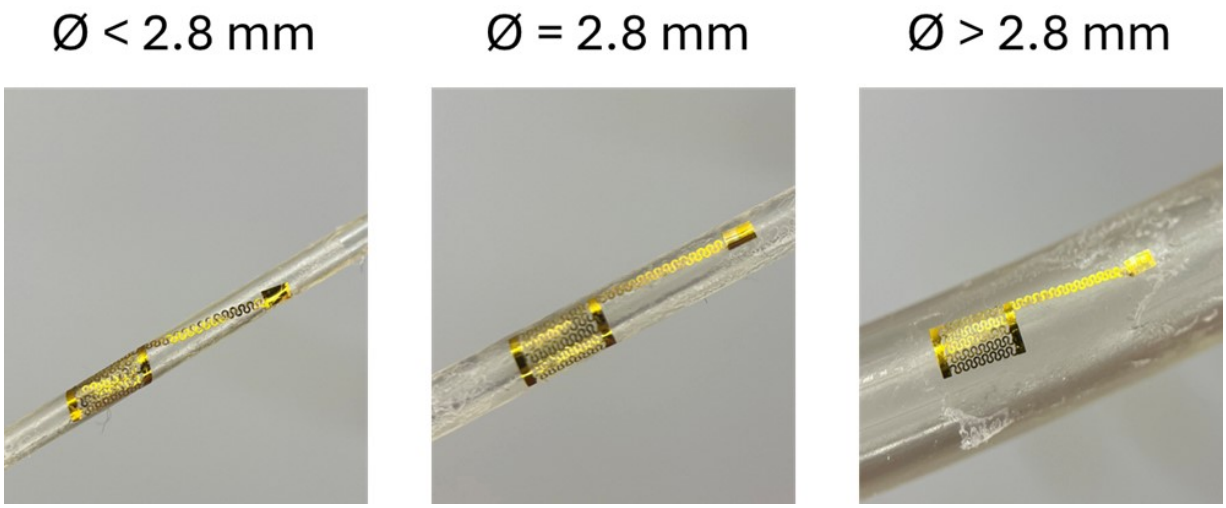

Figure S11 Integration of the serpentine electrodes to a tubular-shaped platform with various diameters, starting from 2 mm to 5 mm. The 2.8 mm is selected as the benchmark diameter because it is the typical dimension of the EVD catheter, the basis of our current design.

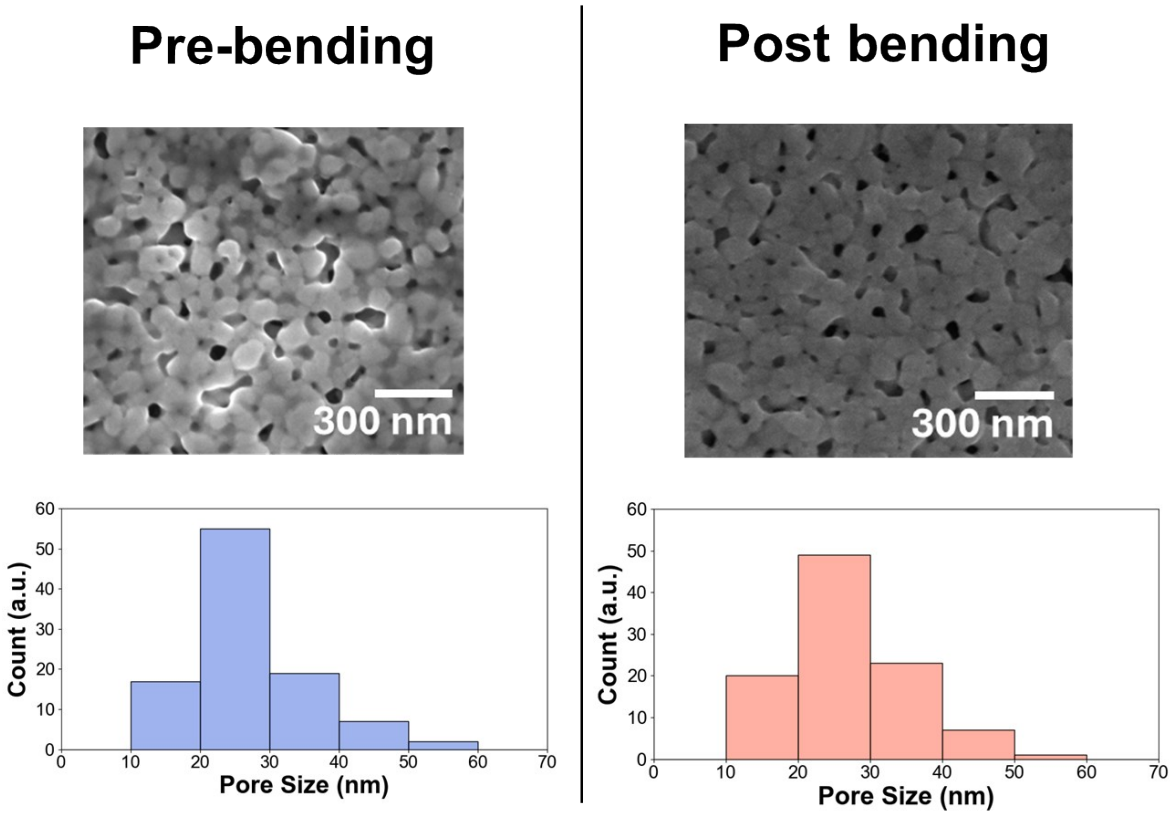

Figure S12 SEM micrographs of mesoporous gold before (pre-bending) and after (post-bending) being subjected to repeated bending cycles (100 cycles). Followed by image analysis for pore size distribution of mesoporous gold.

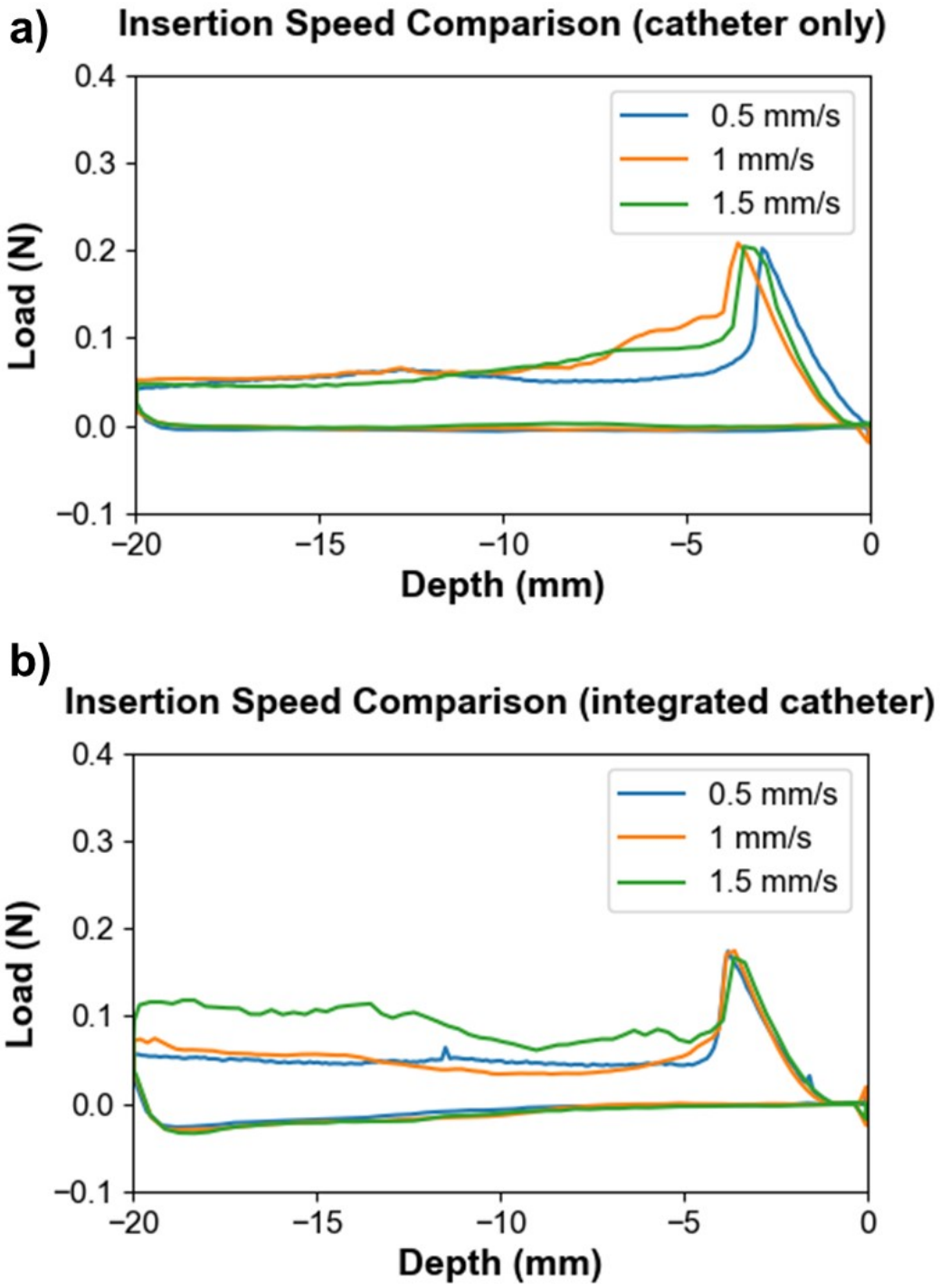

Figure S13 Comparison of insertion force measurement on (a) plain catheter and (b) integrated catheter under different insertion rates

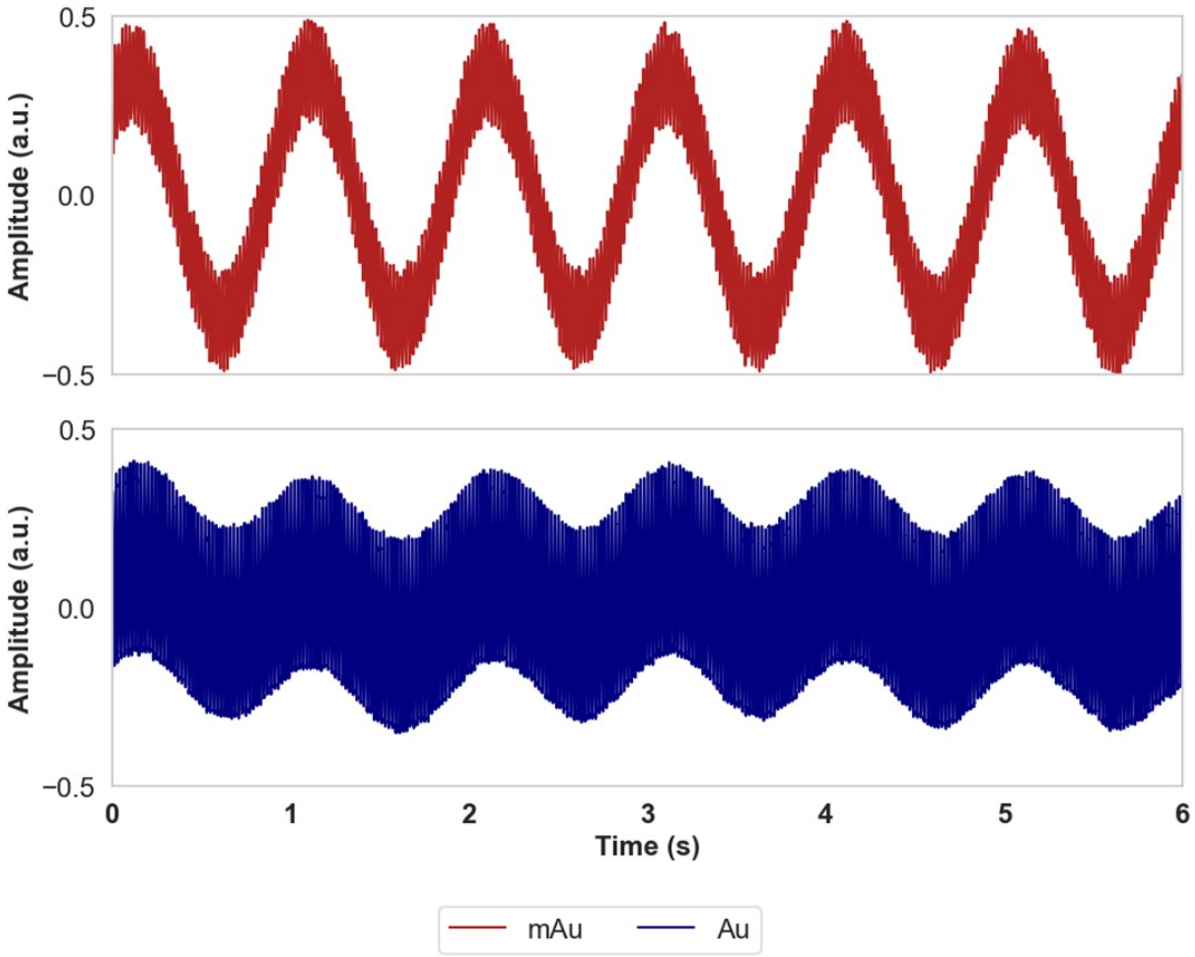

Figure S14 Benchtop characterization comparison of electrode recording capabilities of artificial LFP recording at 1 Hz between mesoporous gold electrodes (top) and flat gold electrodes (bottom).

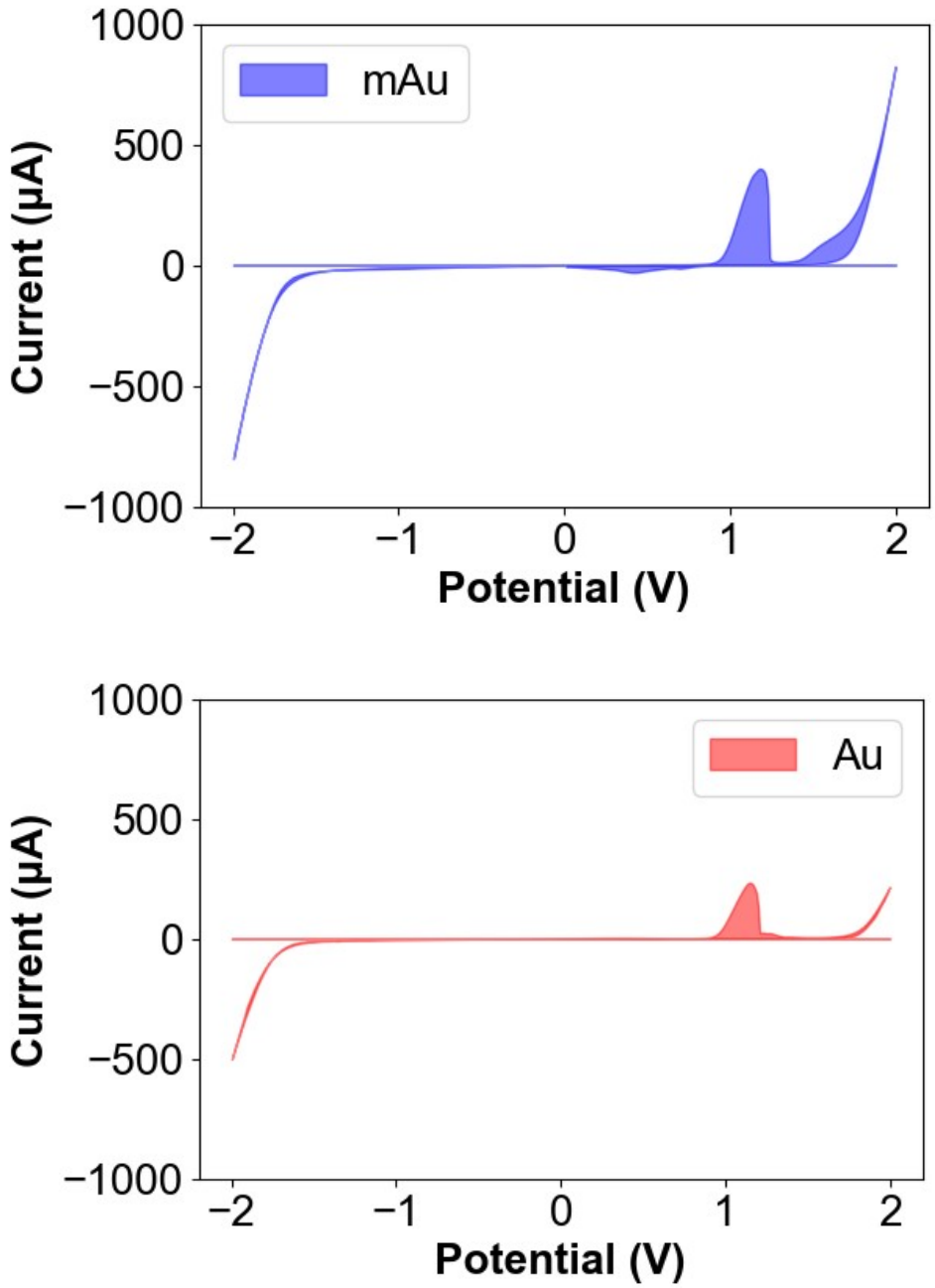

Figure S15 Cyclic voltammetry results of mesoporous gold (top) and flat gold (bottom) in 1x PBS solution

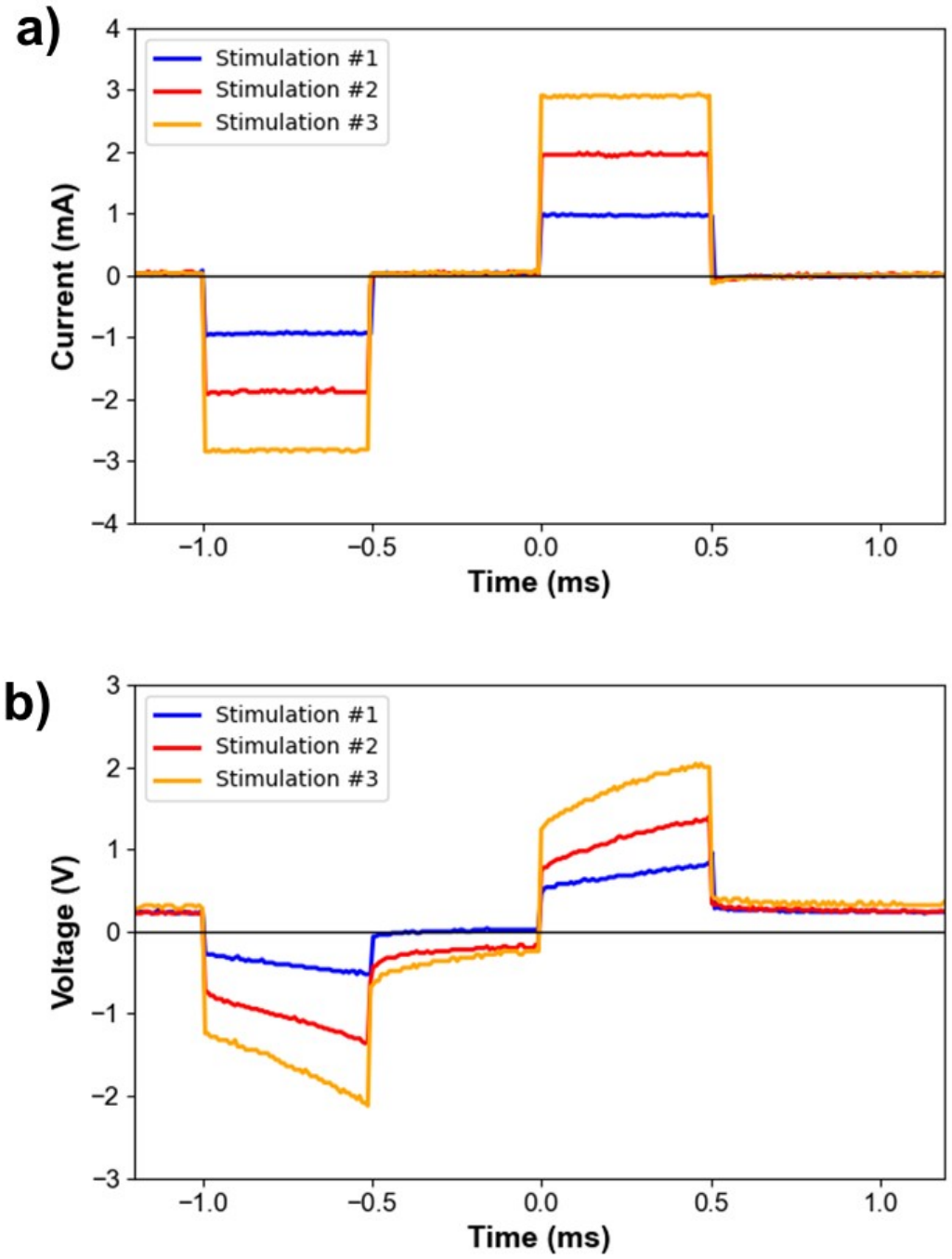

Figure S16 (a) Biphasic stimulation magnitude for characterization of charge injection capacity (b) voltage transient of mesoporous gold electrodes under the corresponding stimulation magnitude.

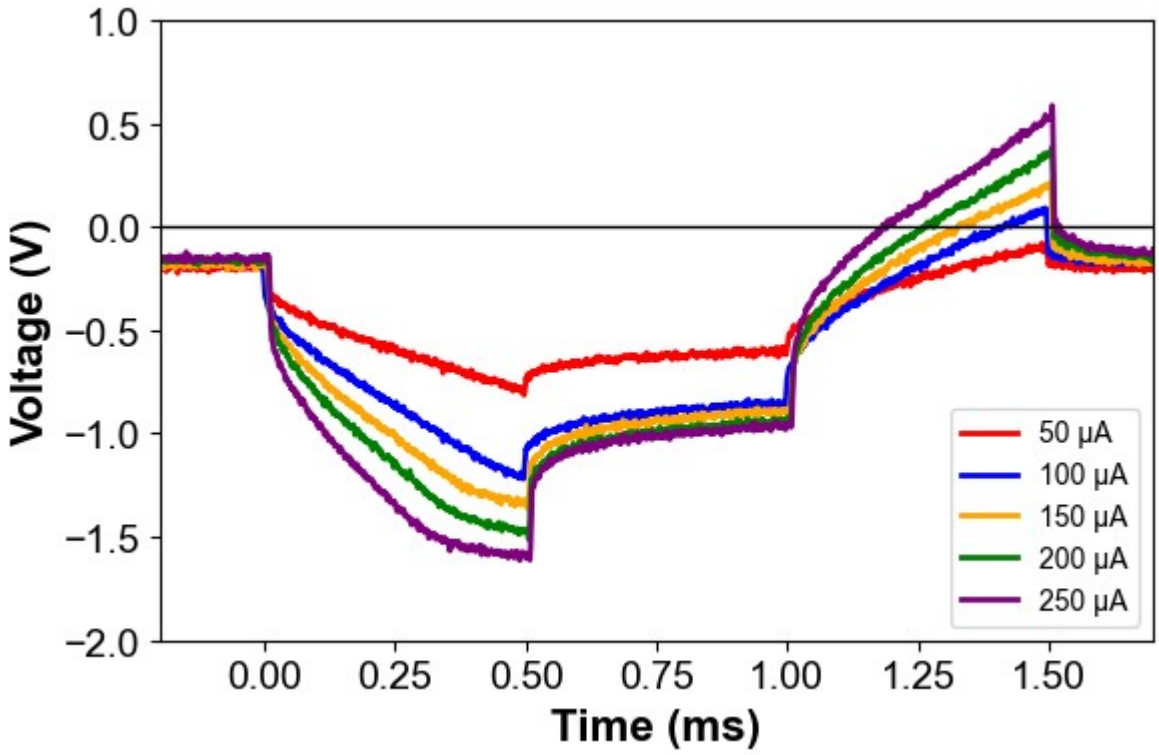

Figure S17 Voltage transient of flat gold electrodes with various cathodic first biphasic stimulation parameters

PI

Properties	Unit	Value
Density	kg/mm3	1.38E-06
Isotropic Elasticity		
Young's Modulus	MPa	2478
Poisson's Ratio	-	0.3986
Bulk Modulus	MPa	4073
Shear Modulus	MPa	885.89
Ultimate Tensile Strength	MPa	92.43
Tensile Yield Strength	MPa	87.88

Gold

Properties	Unit	Value
Density	kg/mm3	1.93E-05
Isotropic Elasticity		
Young's Modulus	MPa	75760
Poisson's Ratio	-	0.42
Bulk Modulus	MPa	1.58E+05
Shear Modulus	MPa	26676
Ultimate Tensile Strength	MPa	199
Tensile Yield Strength	MPa	183.9

Silicone

Properties	Unit	Value
Density	kg/mm3	2.33E-06
Isotropic Elasticity		
Young's Modulus	MPa	1.63E+05
Poisson's Ratio	-	0.27
Bulk Modulus	MPa	1.18E+05
Shear Modulus	MPa	64055
Ultimate Tensile Strength	MPa	172.3
Tensile Yield Strength	MPa	172.3

Table S1. Material properties assigned on FEA analysis using ANSYS Workbench